Hindawi
Geofluids
Volume 2023, Article ID 5157780, 8 pages
https://doi.org/10.1155/2023/5157780

Research Article

Gas and Water Seepage of Tight Gas and Its Application in Well Production Analysis

Rui Zhang, Yang Gao, Yanbin Zhang, Peng Zhang, Xiaoli Pan, Wenjing Yang, Ligang Lv, and Xingguan Chen

The No.1 Gas Plant, Changqing Oilfield of CNPC, Jingbian, China 718500

Correspondence should be addressed to Rui Zhang; gangtie2021@126.com

Received 5 August 2022; Revised 2 October 2022; Accepted 10 October 2022; Published 31 January 2023

Academic Editor: Dengke Liu

Changqing tight gas field has been on fashion among China in recent years. Figuring out gas and water seepage behaviors matters a lot for maximizing gas reservoir recovery. One tool for that is to conduct two-phase seepage experiment and reveal seepage features. Experiments show that gas or water's flowing capacity has a directly positive relationship with its saturation. The larger saturation, the higher permeability. Thus, one method of determining whether a gas well produces water or not is to compare the initial water saturation with its starting-flowing saturation. If the initial gas or water saturation is larger than its critical saturation, it starts to flow. Meanwhile, this critical saturation ranges hugely. For reservoirs with high porosity, permeability, and pore structure like type I, the starting-flowing saturation is 15.6% for gas and 36.6% for water, meaning that it is easily for gas or water to reach the critical saturation and make the seepage happen. The critical saturation in reservoir of type III which has low porosity, permeability, and pore structure is as high as 28.8% for gas and 58.1% for water, indicating that high fluid saturation is needed to have it flow. Finally, four horizontal wells in Sudongnan block are analyzed to verify the method. The prediction that two of them will produce water in the beginning and the other two will not is highly in line with their production data. This method has been proved effective in the prediction of gas wells.

1. Introduction

Tight gas reservoir is known for its perplexed micro features such as small pore radius, bad pore connection, strong seepage disturbance, and serious reservoir heterogeneity [1–4]. These unfavorable features have huge negative impacts on the development of gas field [5, 6]. As an iconic of Sulige gas field, Sudongnan block has established a horizontal-well-featured demonstration area which adopts diverse advanced technologies to further improve the gas field development. During the three years practice, the area has achieved an expected and satisfied success on the development [7–10]. However, some problems still remain unsolved in the gas production [11]. The significant one is that once water flows out of reservoir it is becoming more difficult for horizontal wells to bring water out of well hole than vertical or directional ones. Some wells may see small up and downs of gas production, while others suffer serious drop in production and pressure. Thus, it is vital to figure out the essence of these problems before tackling them. In fact, the output of gas or water results from its microseepage within reservoir [12, 13]. So the idea is to reveal micro properties of the reservoir firstly, then to study the gas-water seepage features, and finally to analyze the production of gas wells.

2. Reservoir Features of Sudongnan

2.1. Reservoir Features of Sudongnan. Located in the southeast of Sulige gas field which belongs to Shaanbei slope, one of five basic units in Ordos basin, Sudongnan is famous for high quality of He8 formation, a favorable gas-bearing reservoir in upper Paleozoic [14]. In Sudongnan, He8 has three main kinds of rock: lithic-quartz sandstone which is dominant, lithic sandstone, and quartz sandstone (see Figure 1). Its porosity changes between 6% and 12%, with the average of 8.7%. The permeability ranges between $0.1 \times 10^{-3}\mu m^2$ and $1.4 \times 10^{-3}\mu m^2$ with the average of

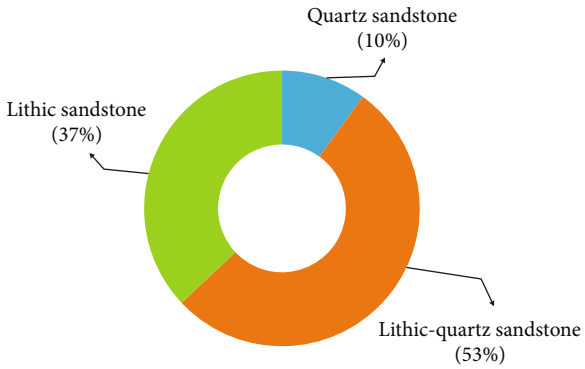

Figure 1: Proportion of three types of rock in He8.

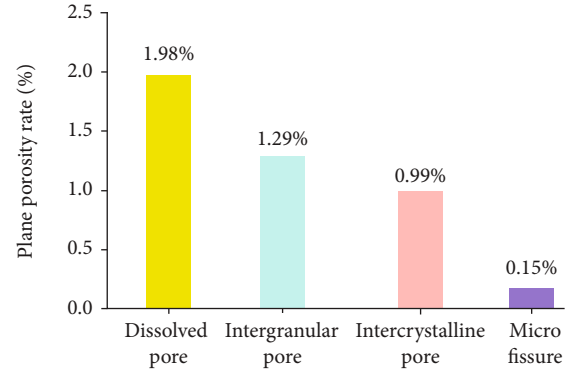

Figure 2: Plane porosity of four types of pores in He8.

$0.55 \times 10^{-3}\,\mu m^2$. He8 has been buried as deeply as about 3080 m where strong diagenesis have taken place and formed very complex pore structure [15]. The current pore types of He8 consist of dissolved pores, residual intergranular pores, intercrystalline pores, and microfissures occasionally (see Figure 2).

3. Experiments and Samples

3.1. Mercury Injection Experiment. In order to obtain pore structure data, mercury is injected into samples at a low and stable speed. The experiment is done by a device called ASPE-730 which is produced by Coretest Systems company [16]. Samples are made with the diameter of 2.5 cm. During the experiment, mercury is injected into samples at the speed of 0.00005 ml/min. Pores are the first space where mercury goes as they are larger than throat in size. With more mercury continuing entering the sample, the injection pressure rises. When it is larger than the capillary pressure, mercury will go through throat and into surrounding pores. At the same time, the injection pressure drops [17]. This is one round of mercury injection, during which the volume of mercury and pressure is recorded to compute parameters of pores and throats: number, radius, and saturation. After rounds and rounds of rise and drop, the parameters of every pore and throat are obtained.

3.2. Gas and Water Seepage Experiment. Gas-water seepage is one kind of multiple-fluid flow which commonly exists in the development of gas field. To make sure experiment data have good representative meanings, 23 samples are selected from gas-producing layers which have been developed by horizontal wells. The experiment is carried out under unstable state. Firstly, samples are fully saturated by water under the surface condition of pressure and temperature. Then, nitrogen is injected into samples to drive water out with a stable speed until no more water flows out. Secondly, nitrogen and water saturation are tested together with their permeability. Thirdly, water is injected to drive nitrogen, during which another set of saturation and permeability data is gained (see Figure 3).

4. Experiment Results

4.1. Pore and Throat. According to the data of 11 samples (see Table 1), the difference between pore and throat is apparent. For all samples, there is little difference in pore size mainly ranging from 100 μm to 200 μm (see Figure 4). The major difference may be the peak proportion of pore size. Some samples' pore size peaks at 120 μm, while others at 170 μm. No matter what size the pore proportion peaks, the top proportion is from 11% to 27%. Small difference in pore size and proportion among these 11 samples implies that the dominant factor of defining reservoir quality may not be pore size.

According to throat radius distribution curves (see Figure 5), throat size mainly ranges from 0.2 μm to 1.8 μm. Unlikely to pores, throats show obvious differences. Major throat size varies hugely from one sample to another. For samples with low porosity and permeability, throats are made up of smaller ones with radius between 0.2 μm and 0.5 μm. However, other samples which are higher in porosity and permeability have a wide range of throats scattering from 0.6 μm to 1.6 μm. The dominant proportion of throat radius changes largely, from 11% to 53%. The big difference in prime proportion suggests that throat size plays a dominant role reservoir quality (see Table 1).

4.2. Gas and Water Seepage. It is obvious that gas or water's seepage capability has a positive trend with saturation. With gas flowing out, the saturation decreases for gas and increases for water. When water saturation rises up beyond its critical saturation, water will come out too. As more and more gas flows out of samples, relative permeability decreases rapidly for gas and increases for water. The focus of these experiments is on the critical saturation where gas or water starts flowing. Gas critical saturation (hereinafter referred to as "S_g (gf)") is the diving saturation, beyond which gas starts flowing and within which gas stops flowing. Water critical saturation (hereinafter referred to as "S_w(gf)") is the dividing saturation, beyond which water starts flowing and within which water stops flowing [18]. Thus, whether a gas-bearing layer produces water or not can be determined by comparing its initial saturation with critical saturation.

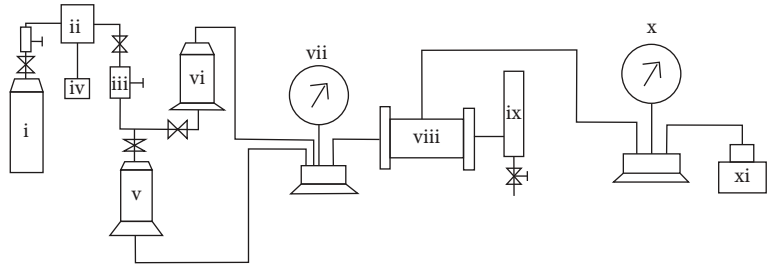

Figure 3: Diagram of nitrogen and water seepage experiment. (i) Air source, (ii) injection pump, (iii) adjusting valve, (iv) buffer bottle, (v) water bottle, (vi) nitrogen bottle, (vii) injection pressure gauge, (viii) sample, (ix) separator, (x) surrounding pressure gauge, and (xi) surrounding pump.

Table 1: Porosity, permeability, pore, and throat of 11 samples.

Samples	Depth (m)	Porosity (%)	Permeability ($\times 10^{-3}\mu m^2$)	Main pore radius (μm)	Main throat radius (μm)
1#	3137.56	9.1	0.112	145.9	0.791
2#	3051.60	12.8	0.521	152.4	1.263
3#	3082.46	11.2	0.312	156.2	0.857
4#	3141.50	10.9	0.453	149.6	1.329
5#	3097.84	9.8	0.212	142.8	0.613
6#	3069.18	7.9	0.147	139.8	0.733
7#	3098.21	7.3	0.129	159.2	0.665
8#	3113.21	12.5	0.853	134.9	1.681
9#	3097.12	12.7	0.359	117.8	0.729
10#	3133.25	8.1	0.219	121.3	0.541
11#	3107.93	6.2	0.115	142.8	0.368

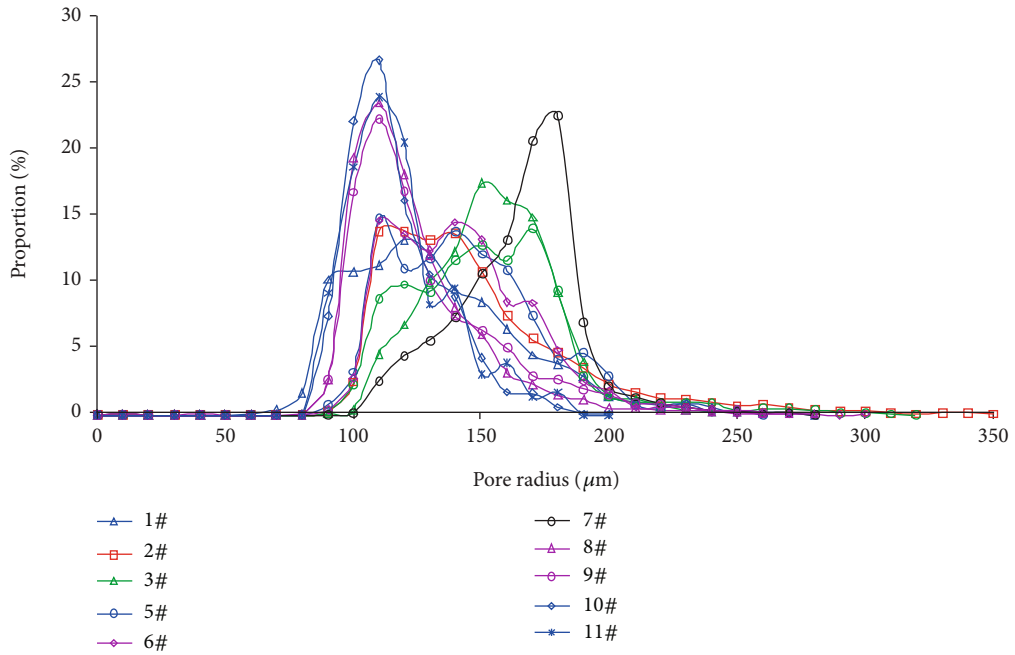

Figure 4: Probability curves of pore radius from 11 samples of He8.

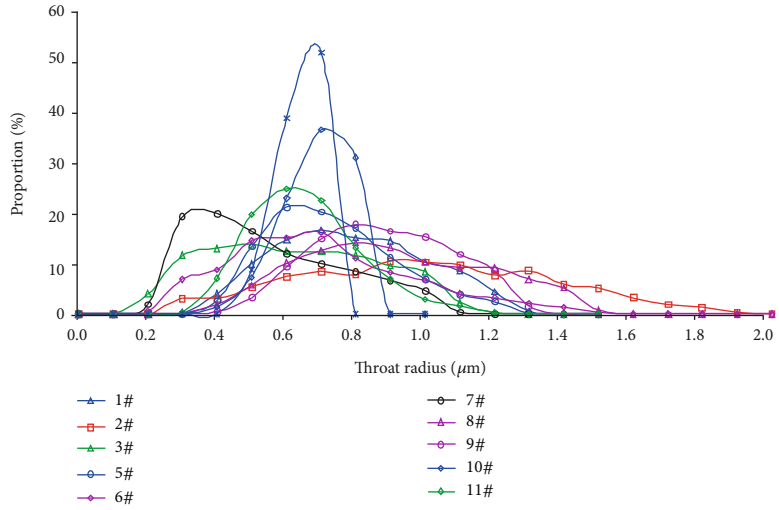

Figure 5: Probability curves of throat radius from 11 samples of He8.

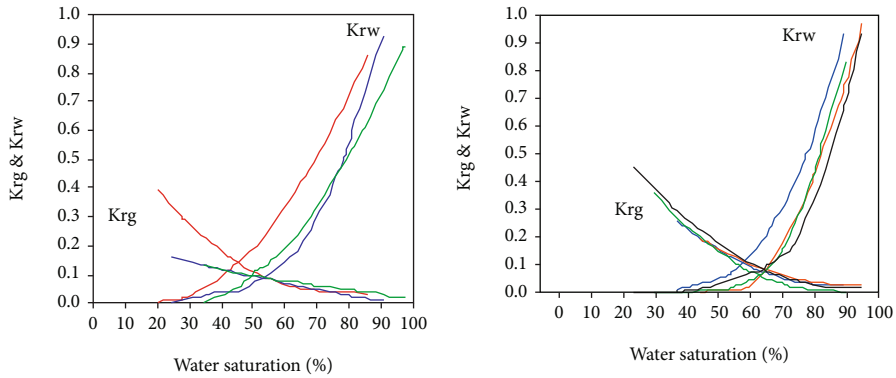

(a) Seepage curves of type I

(b) Seepage curves of type II

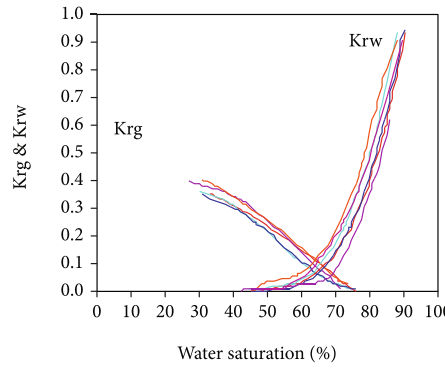

(c) Seepage curves of type III

Figure 6: Three kinds of seepage curves in He8. (a) Seepage curves of type I. (b) Seepage curves of type II. (c) Seepage curves of type III.

This is basic principle of applying gas and water seepage experiment in gas well production prediction.

In order to clearly understand gas and water seepage features of He8, all samples are classified into three types according to the saturation range where water and gas can flow together (see Figures 6(a)–6(c)). Type I has the wide range of saturation while Type III has the narrow range. The wide range means the small critical saturation and high common flow possibility.

Gas or water's seepage capability has a close relationship with porosity, permeability, and pore size (see Table 2). The larger these parameters are, the lower fluid critical saturation is. Thus, reservoirs with better qualities have a lower critical saturation, indicating that higher gas saturation is required to ensure production without water. Thus, high porosity and permeability are double swords for normal production.

Table 2: Reservoir parameters and critical saturation of three different types of seepage curves.

Type	Average Porosity	Average Permeability	Throat size		Critical saturation	
			Main range	Peak range	S_g(gf)	S_w(wf)
I	9.3%	$0.53 \times 10^{-3}\mu m^2$	0.2-4.4 μm	1.24 μm	15.6%	36.6%
II	8.7%	$0.47 \times 10^{-3}\mu m^2$	0.2-0.8 μm	0.32 μm	21.4%	49.5%
III	7.6%	$0.33 \times 10^{-3}\ \mu m^2$	0.1-0.3μm	0.24 μm	28.8%	58.1%

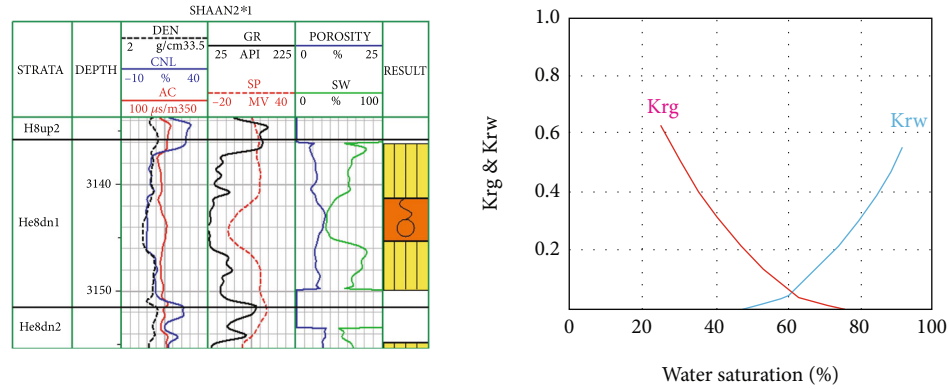

(a) He8's electrical logging interpretation of Shaan2*1 (b) Seepage curve of sample 4#

Figure 7: He8's electrical logging interpretation and seepage curve of Shaan2*1. (a) He8's electrical logging interpretation of Shaan2*1. (b) Seepage curve of sample 4#.

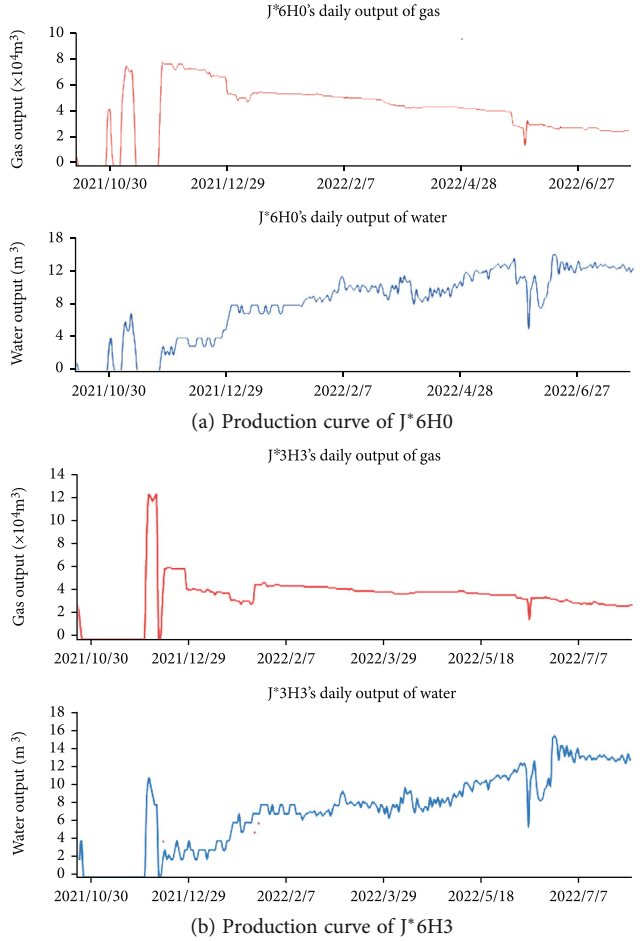

(a) Production curve of J*6H0

(b) Production curve of J*6H3

Figure 8: Production curves of two horizontal wells on Shaan2*1 well group. (a) Production curve of J*6H0. (b) Production curve of J*6H3.

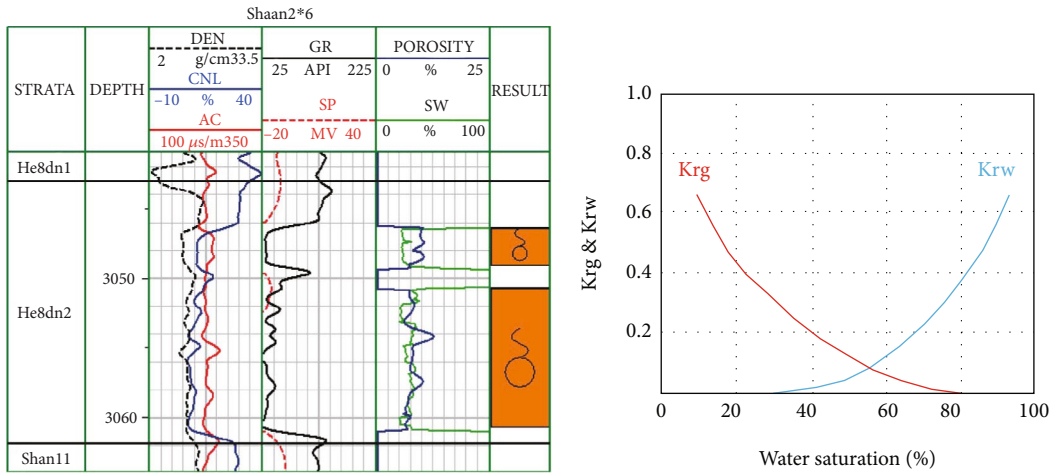

(a) He8's electrical logging interpretation of Shaan2*6

(b) Seepage curve of sample 2#

Figure 9: He8's electrical logging interpretation and seepage curve of Shaan2*6. (a) He8's electrical logging interpretation of Shaan2*6. (b) Seepage curve of sample 2#.

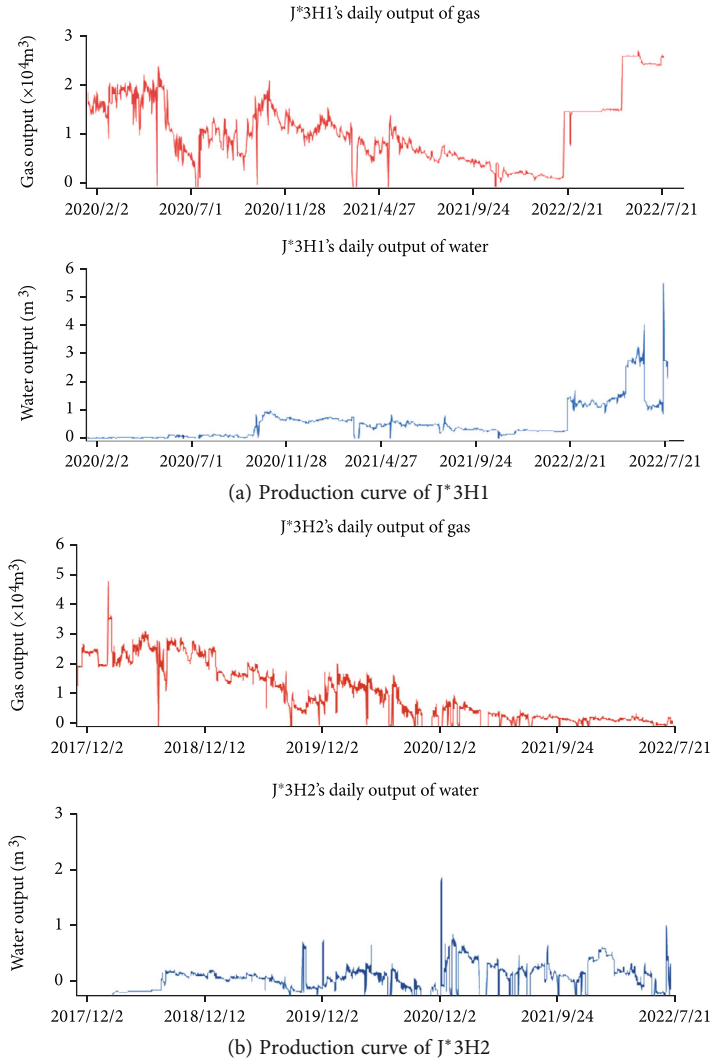

(a) Production curve of J*3H1

(b) Production curve of J*3H2

Figure 10: Production curves of two horizontal wells on Shaan2*6 well group. (a) Production curve of J*3H1. (b) Production curve of J*3H2.

5. Application in Production Analysis

5.1. Brief Introduction of Horizontal Wells. Because of having only one gas-bearing layer developed, horizontal wells are the best choice to verify experiment results. Generally speaking, horizontal wells in Sudongnan have two directions: northward and southward. So one target layer often has two horizontal wells drilled. Here, four horizontal wells at two well groups which have two samples tested are discussed.

*5.2. Horizontal Wells: J*6H0 and J*6H3.* Two wells stand on the well group: Shaan2*1 which has sample 4# tested at the depth of 3141.5 m. Around the sample depth, He8 develops a gas layer of 3.5 m thick (see Figure 7(a)). Electrical logging interprets that the gas saturation ranges between 15.4% and 62.9%, with the average of 46.8%, and the average water saturation is 53.2%. From the seepage curve of Sample 4#, the water critical saturation is 47.9%, and the curve shape is alike type II (see Figure 7(b)). It is expected that two wells are about to produce water at early stage because the initial water saturation is larger than its critical saturation. In fact, two horizontal wells produced about 5.0 m^3 water every day since the first day of opening, and the output of water rose to 10.0 m^3/d one month later (see Figures 8(a) and 8(b)). The production feature responds well with the expectation. The suggestion for gas wells of this kind is that the formation pressure should be controlled and utilized to bring water out of well hole.

*5.3. Horizontal Wells: J*3H1 and J*3H2.* Two wells stand on the well group: Shaan2*6 which has sample 2# tested at depth of 3051.6 m. Around the sample depth, there develops a gas layer of 12.4 m thick (see Figure 9(a)). Electrical logging interpretation shows that gas saturation mainly ranges between 61.9% and 80.2%, with the average of 71.6%, and the average water initial saturation is about 28.4%. From the seepage curve of sample 2# which is type I, the water critical saturation is around 32.1% (see Figure 9(b)). Thus, there is an expectation that no water will show at early stage because the initial water saturation is lower than its critical saturation. Two horizontal wells produced natural gas without water at early sage. About one half year later, they start seeing water flowing out of well hole with output of 1.0 and 0.5 m^3 every day (see Figures 10(a) and 10(b)).

6. Conclusions

(1) The permeability of tight sandstone is subject to throats while not pores. The larger the throat, the higher the permeability. Constant mercury injection experiments demonstrate that throat radius ranges from 0.2 μm to 1.8 μm, and pore radius mainly ranges from 100 μm to 200 μm

(2) Gas and water seepage experiment is an effective method of obtaining the critical saturation. If the initial water saturation is larger than its critical saturation, gas wells will see water in early production. The idea has been proved reliable by four horizontal wells. The critical saturation is mainly dependent on pore structures and varies hugely. The better reservoir parameters are, the higher seepage capability gas or water has. Higher gas saturation is necessary to prevent gas wells from producing water when reservoir has high permeability and large pores. If the initial gas saturation is less than its critical point, reservoir formation pressure should be highly utilized to keep gas wells production normal and longer

(3) Complexity and heterogeneity of pore structure and fluid seepage are severe in tight gas reservoir. One set of sandstone can be divided into several subsections where differences are obvious in pore, throat, and initial saturation. Some subsection may not produce while others are bound to see water at early stage. If one of subsections has the large possibility of producing water, the whole sandstone should be seen as highly risk. All subsections should be included in the calculation of the initial water saturation. At the same time, fracturing design should take full consideration of those important differences

Data Availability

All data generated or analyzed during this study are included in this article.

Conflicts of Interest

The authors declare that the paper does not have any conflict of interest with other units and individuals.

Acknowledgments

The work was supported by National Science and Technology Major Project "Demonstration Project for Development of Large-scale Low Permeability Lithologic Reservoir in Ordos Basin" (Number 2016ZX005050).

References

[1] R. Zhang, *Detailed Study on Gas-Water Relative Flow of Tight Gas Sandstone: A Case from He8 Formation of Southeastern Sulige Area*, Northwest University, 2014, Master's Dissertation.

[2] H. X. Wei, *Study on the Morphology of Tight Gas Reservoir Gas-Water Relative Permeability Curve and the Characterization of Permeability Jail*, China University of Geoscience for Master Degree, 2021, Master's Dissertation.

[3] J. W. Tang, A. L. Jia, D. B. He et al., "Development technologies for the Sulige gas field with low permeability and strong heterogeneity," *Petroleum Exploration and Development*, vol. 1, pp. 107–110, 2006.

[4] Y. Yang, S. P. Da, and X. R. Xu, "Pore structure study of $P_{1\text{-}2}sh^8$ reservoir in Sulige gasfield," *Natural Gas Industry*, vol. 25, no. 4, pp. 50–52+9, 2005.

[5] H. H. Liu, Y. H. Cui, S. C Xia et al., "Occurrence mechanism of formation water in Shihezi8 and Shanxi1 tight gas reservoirs and its main control factors: an example from one block in Sulige gasfield," *Natural Gas Exploration and Development*, vol. 43, no. 1, pp. 84–91, 2020.

[6] Sh. X. Lu, R. H. Yan, and X. M. Yuan, "Reservoir characteristics and controlling factors of He8 member, southern Sulige gasfield," *Natural Gas Exploration and Development*, vol. 35, no. 3, pp. 1–4+81, 2012.

[7] H. Wang, Y. H. Cui, X. L. Liu, Z. Z. Qiang, and S. C. Wang, "Multi-layer horizontal wells development for tight sandstone gas reservoir: case study of tight gas reservoir model in Ordos basin," *Natural Gas Geoscience*, vol. 32, no. 4, pp. 472–480, 2021.

[8] S. X. Fei, D. X. Wang, G. Lin, X. Pan, Y. Wang, and B. Zhang, "The key geological technology for horizontal wells overall development in tight sandstone gas reservoirs: take the Sudongnan area of Sulige gasfield for an example," *Natural Gas Geoscience*, vol. 25, no. 10, pp. 1620–1629, 2014.

[9] J. C. He, H. J. Yu, G. H. He, J. Zhang, and Y. Li, "Natural gas development prospect in Changqing gas province of the Ordos basin," *Natural Gas Industry*, vol. 41, no. 8, pp. 23–33, 2021.

[10] S. X. Fei, H. J. Yu, C. L. Chen, L. A. Zhu, X. L. Liu, and Y. J. Wang, "Key technologies to development of tight sandstone gas reservoir by horizontal wells: a case study on the upper Paleozoic gas reservoir in Sulige gasfield," *Journal of Xi'an Shiyou University*, vol. 37, no. 4, pp. 26–35, 2022.

[11] E. Ye, *Investigation of the Water Production Effect on Gas Well Productivity in Sulige Gasfield*, China University of Petroleum, 2018, Master's Dissertation.

[12] H. T. Zhang, Z. Shi, Z. L. Ren, and M. Li, "Characteristics of water bearing-formation and gas-water distribution control factors in gas reservoir He8 of Sulige gasfield, Ordos Basin," *Geoscience*, vol. 25, no. 5, pp. 931–937, 2011.

[13] Y. Ch. Li, "Gas-water percolation law of tight sandstone reservoirs with different pore types in the middle and northern Sulige gasfield," *Unconventional Oil & Gas*, vol. 9, no. 5, pp. 69–78, 2022.

[14] Z. X. He, J. H. Fu, Sh. L. Xi, S. T. Fu, and H. P. Bao, "Geological features of reservoir formation of Sulige gasfield," *Acta Petrolei Sinica*, vol. 2, pp. 6–12, 2003.

[15] Q. S. Wei, K. Y. Wei, Z. Li et al., "Diagenesis and porosity evolution of tight sandstone gas reservoirs in the Western Sulige area, Ordos basin," *Geology and Exploration*, vol. 57, no. 2, pp. 439–449, 2021.

[16] H. Gao, W. Xie, J. P. Yang, C. Zhang, and W. Sun, "Pore throat characteristics of extra-ultra low permeability sandstone reservoir based on constant-rate mercury penetration technique," *Petroleum Geology & Experiment*, vol. 33, no. 2, pp. 206–211 +214, 2011.

[17] D. J. Feng and K. H. Xiao, "Constant velocity mercury injection and nuclear magnetic resonance in evaluation of tight sandstone reservoirs in Western Sichuan basin," *Petroleum Geology & Experiment*, vol. 43, no. 2, pp. 368–376, 2021.

[18] W. Ji, "Gas water relative flow of tight sandstone gas reservoirs and its influences factors: case study of member 8 of Permian Xiashihezi formation and member 1 of Permian Shanxi formation in Shaan well 234-235 area of Sulige gas-field in Ordos basin," *Journal of Jilin University (Earth Science Edition)*, vol. 49, no. 6, pp. 1540–1554, 2019.